This material has been copied
under licence from CANCOPY.
Resale or further copying of this material is
strictly prohibited.

Le présent document a été reproduit
avec l'autorisation de CANCOPY.
La revente ou la reproduction ultérieure
en sont strictement interdites.

Dr. J. Slater

Neutron Behavior in Cluster-Type Fuel Lattices, (II)

Theory and Analysis of Experiment

Kazuko YAMAMOTO, Kunitoshi KURIHARA, Masayoshi ISHIDA,
Ken-ichi MATSUOKA and J. Tsunetaka WAJIMA

Reprint

Journal of NUCLEAR SCIENCE and TECHNOLOGY, Vol. 9, No. 12, pp. 705~715, December 1972
A Publication of the ATOMIC ENERGY SOCIETY OF JAPAN

Journal of NUCLEAR SCIENCE and TECHNOLOGY, 9(12), p. 705~715 (December 1972).

Neutron Behavior in Cluster-Type Fuel Lattices*, (II)

Theory and Analysis of Experiment

Kazuko YAMAMOTO, Kunitoshi KURIHARA, Masayoshi ISHIDA, Ken-ichi MATSUOKA and J. Tsunetaka WAJIMA

*Atomic Energy Research Laboratory, Hitachi Ltd.***

Received October 6, 1971
Revised March 2, 1972

A multigroup method of calculation is presented for describing the neutron behavior in a cluster-type fuel lattice. It solves the integral transport equation by a semi-analytical method proposed in a previous paper for calculating collision probabilities in the lattice of a clustered fuel element. Using only fundamental nuclear data, it gives space and energy dependent neutron flux. The method has been programmed for HITAC-5020F (computer code named CLUSTER-III).

The accuracy of the method has been tested by comparing the calculation with the experiment described in Part (I) of this paper. The lattices are 28-pin clusters of UO_2 or PuO_2+UO_2 fuel pins, with heavy- or light-water moderators and with light-water coolant containing varying void ratios. The quantities studied are micro-parameters, reaction distributions in energy and space, thermal disadvantage factors and the multiplication factors. It is found that the calculated results are generally in good agreement with experiment, typically within 10% for micro-parameters and thermal disadvantage factor, and within 1% for the multiplication factor.

KEYWORDS: ***neutron behavior, cluster-type fuel lattices, multigroup method, semi-analytical collision probability method, neutron flux, neutron transport theory, uranium dioxide, plutonium dioxide, reactor lattice parameter, mixture, fuel pins, voids, multiplication factors***

I. INTRODUCTION

The behavior of neutrons in a cluster-type fuel lattice is complex because of its highly heterogeneous structure in a unit cell geometry. This heterogeneity affects the various parameters of the reactor, such as power peaking and void coefficient. It will be a key problem in a cell calculation of this type of reactor to represent the heterogeneity effect on reactor parameters with necessary precision.

Several approaches have been proposed so far[(1)~(3)]. Most of them are based, more or less, on collision probability. The validity of these approaches depends on the availability of an accurate and fast method to calculate collision probabilities. Previously, two of the authors have proposed a semi-analytical method for calculating collision probabilities in cluster-type fuel lattices[(4)]. The values obtained with this method have been compared with exact numerical method, with favorable results.

In this paper a multigroup method of calculation dealing with a unit cell of a clustered fuel element is presented with the above mentioned semi-analytical method for calculating collision probabilities. It solves coupled integral transport equations using fundamental nuclear data and obtains the space dependent neutron flux through the neutron life cycle. Using the neutron flux thus obtained it yields energy integrated or averaged quantities such as micro-parameters, few group constants, and multiplication factor. The method has been programmed for the HITAC-5020F (computer code CLUSTER-III). The accuracy of the method is tested by comparing the results of the calculation with those of experiments, the details of which are reported in Part (I) of this paper.

* The work partially supported by a contract between the Power Reactor and Nuclear Fuel Development Corporation (PNC) and Hitachi Ltd.

** *Ozenji, Kawasaki-shi.*

II. Method of Calculation

1. Basic Equation

Starting from the integral form of the time independent Boltzmann transport equation, the basic equation of the collision probability theory can be obtained as follows[5].

Let $\phi(\vec{r}, E, \vec{\Omega})$ be the neutron angular flux. The integral transport equation is, then,

$$\phi(\vec{r}, E, \vec{\Omega}) = \int \frac{d\vec{r}'}{4\pi|\vec{r}-\vec{r}'|^2} e^{-\tau(\vec{r}', \vec{r}, E)} S(\vec{r}' E, \vec{\Omega}), \quad (1)$$

where $S(\vec{r}, E, \vec{\Omega})$ is the total neutron source density at the space point $\vec{r}$, at energy E and in the direction $\vec{\Omega}$. In general, $S(\vec{r}, E, \vec{\Omega})$ contains fission, scattering and external sources; $\tau(\vec{r}', \vec{r}, E)$ is the optical length between the space points $\vec{r}'$ and $\vec{r}$ for a neutron of energy E.

Consider an infinitely extended periodic lattice, and subdivide a unit lattice cell into N small sub-regions. In each of the small regions the nuclear cross section is assumed constant. Under this assumption the integral transport equation is reduced to a set of N coupled transport equations:

$$V_n \Sigma_n(E) \bar{\phi}_n(E) = \mathop{S}_{m=1}^{N} V_m P_{mn}(E) \bar{S}_m(E), \quad (2)$$
$$(n=1, 2, \cdots N)$$

where $\bar{\phi}_n(E)$ and $\bar{S}_n(E)$ are integrated with respect to angle, the region-average neutron flux and the region-average neutron source density in sub-region n, respectively; V_n is the volume of a small sub-region n, and $\Sigma_n(E)$ the total cross section in the sub-region n, at energy E; $P_{nm}(E)$ denotes the probability for a neutron of energy E born in a sub-region n to undergo its first collision in a sub-region m. This quantity depends on the source distribution, but for the sake of simplicity, the flat flux and isotropic scattering approximations are usually adopted:

$$P_{nm}(E) = \frac{\int_{r \in V_n} d\vec{r} \, \Sigma_n(E) \int_{r' \in V_m} d\vec{r}' \frac{1}{4\pi|\vec{r}-\vec{r}'|^2} e^{-\tau(\vec{r}', \vec{r}, E)}}{V_m} \quad (3)$$

Equation (2), together with Eq. (3), are the basic equations of collision probability theory. The source density is expressed more explicitly in the form

$$S_m(E) = \chi(E) \int_0^\infty \nu \Sigma_{fm}(E') \phi_m(E') dE' + \int_0^\infty \Sigma_{sm}(E' \to E) \phi_m(E') dE' + Q_n(E). \quad (4)$$

Here, $\Sigma_{fm}(E)$ is the fission cross section in a sub-region m at energy E, and $\chi(E)$ is the distribution of fission neutrons; $\Sigma_{sm}(E \to E')$ is the scattering kernel in a region m, and $Q_m(E)$ is the external source supplied from outside to the system considered. In a self-sustaining system, $Q_m(E)$ must be zero. To perform the numerical calculation, E, the continuous variable of energy is changed into the discrete variable g, say group g. Equations (2) and (4) are thus reduced to:

$$V_n \Sigma_n^g \phi_n^g = \mathop{S}_{m=1}^{N} V_m P_{mn}^g S_m^g \quad (5)$$

$$S_m^g = \chi^g \mathop{S}_{g'=1}^{G} \nu \Sigma_{fm}^{g'} \phi_m^{g'} + \mathop{S}_{g'=1}^{G} \Sigma_{sm}^{g' \to g} \phi_m^{g'} + Q_m^g \quad (6)$$

where Σ_n^g and other cross sections are averaged, and the neutron flux ϕ_n^g is integrated over the energy interval ΔE^g belonging to group g. Collision probabilities are calculated group-wise.

2. Collision Probabilities in Cluster-Type Fuel Lattices

Although Eq. (3) can be solved without any knowledge of flux, it is not so easy to obtain the numerical values of collision probabilities for lattices of complex geometry like those of cluster-type fuel element. Approximations must therefore be necessary. Let the clustered fuel region be subdivided into concentric annuli, numbered outwards from 1 up. Each fuel annulus contains fuel pins and associated coolant (**Fig. 1**). Cladding of the fuel pin is permissible. Each boundary of the fuel annulus is so chosen as to give an equal amount of coolant to each fuel pin. The fuel region is surrounded by homogeneous annular regions.

The collision probability is calculated for a neutron proceeding from one sub-region to another. The fuel annulus from which a neutron starts is treated accurately by taking into consideration the non-uniform structure of the annulus using the

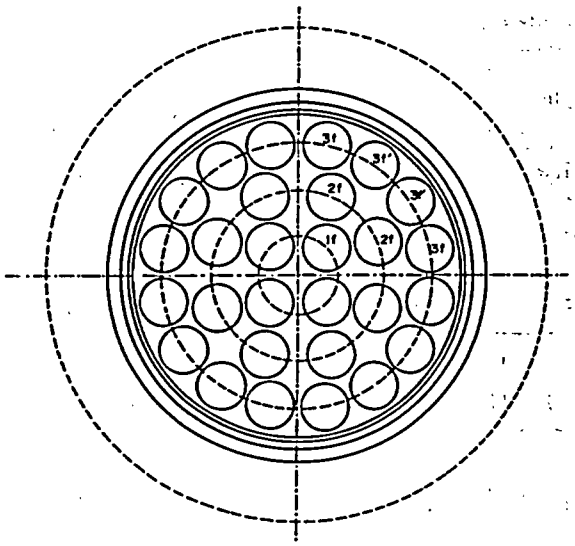

Fig. 1 Unit lattice of 28-pin cluster

subcell model. The other fuel annuli, however, are treated approximately as if it were homogeneous annuli. Homogenized cross sections of the annuli are so determined that the number of outgoing neutrons from the homogenized annuli is equal to that from the actual non-uniform fuel annuli. The collision probability is then partitioned among fuel pins and coolant in the annulus. A detailed description of the methed is found in the previous paper[4].

3. Multigroup Calculation Scheme

In the method presented here, a 69-energy group scheme is adopted. The group constants for this scheme are assumed to be independent of the weighting spectra used to generate them, except the thermal group (the 69-th group of the scheme) constants and the resonance cross sections. These are calculated space-point-wise for each case prior to the 69-group calculation, using the same type of equations as Eqs. (5) and (6) in each restricted energy interval[6]~[9].

In order to obtain the weighting spectra for effective thermal group constants, Eq. (5) is solved in the energy region below E_1 with fundamental library data of 30 groups[6]. The upper boundary E_1 of the weighting thermal spectrum must be chosen sufficiently large so that only few neutrons scatter up across E_1. The first term of Eq. (6) is set to zero, and Q_n^g represents the source of epithermal neutrons above E_1. The scattering kernel in this case is the thermalization kernel. Group constants are obtained by energy integration within the thermal energy region between 0 and $E_c(E_c<E_1)$. The thermal cut-off energy E_c is given as input data.

For the resonance absorption of heavy nuclei contained in the fuel, the flux varies so rapidly even in one group that effective cross sections must be obtained by including more detailed information on the flux within a resonance level. For this purpose, Eq. (5) is solved for each resonance level[7][8] with much finer energy intervals, where g is to be read as energy mesh instead of group. The following assumptions are adopted:

(1) Resonance levels are treated separately.

(2) The neutron flux has an asymptotic form $(1/E)$ at the top energy of each resonance level.

(3) Resonance absorbers and moderating nuclei in the fuel are treated with narrow or wide resonance approximations, or purely numerically, according to the character of the resonance level, but other nuclei outside the fuel are all treated with narrow resonance approximation.

With the resonance flux thus obtained, the effective cross sections of group g of the 69-group scheme become

$$\sigma_{xi}^{g,l}=\underset{E\in g}{S}\sigma_x^g(E)\phi_i^l(E)/\underset{E\in g}{S}\phi_i^l(E), \qquad (7)$$

where l and i denote resonance level and space point, respectively and x is fission or absorption, and E means energy mesh. The statistical model is used for the unresolved resonance region and the effect of the cluster is considered in the form of Dancoff factor, which is calculated from P_{nm}. The values of the calculated resonance integrals for infinite dilution are compared in **Table 1** with those of experiment. It shows that the fundamental data used in the calculations are consistent with experiment.

The neutron leakage effect on the spectrum is included under the assumptions of fundamental buckling mode B and of diffusion approximation. The absorption cross section Σ_{ai} of the region i is replaced by $\Sigma_{ai}+DB^2$. The diffusion constant D of the lattice, while it will be finally obtained by the Benoist method, is obtained provisionally from the volume average in the lattice.

The neutron flux distribution over the whole energy range in a lattice of cluster geometry is

Table 1 Resonance integral (RI^{∞} barn)

Isotope	Reaction	Resonance integral		higher	$1/v$ (>0.5 eV)	RI^{∞}	
		Resolved	Unresolved			CLUSTER-III	Exp. (*BNL*-325)
^{235}U	f	92.2	112.7	17.9	40.3	263.1	274±10
^{238}U	c	272.2	2.0	2.7	1.2	278.1	280±12
^{239}Pu	f	136.1	80.2	21.1	97.8	335.2	335±15
^{240}Pu	c	8378.0	50.9	0.4	9.3	8438.6	8280†
^{241}Pu	f	254.0	165.4	20.2	75.8	515.4	537±27

† DRAKE, M. K.: *Nucleonics*, 108 (Aug. 1966)

Table 2 Experimental and calculated values of ^{238}U resonance integral for 19-pin clusters

Position \ Coolant	H_2O			D_2O			Air		
	Exp.[19]	Cal. 1	Cal. 2	Exp.[19]	Cal. 1	Cal. 2	Exp.[19]	Cal. 1	Cal. 2
1f	12.94	15.35	13.71	10.75	12.48	12.18	9.59	10.78	10.78
2f	13.12	15.44	13.92	11.11	12.77	12.55	10.20	11.18	11.18
3f	13.93	16.66	15.31	13.43	14.90	14.50	12.53	13.63	13.63
3f′	14.41			14.20			13.91		
Av.	13.8±0.3	16.21	14.81	12.8±0.3	15.30	13.80	12.1±0.3	12.71	12.71

Cal. 1: Isotropic scattering only
Cal. 2: Includes anisotropic scattering approximately with transport correction

obtained by solving Eq. (5) with effective thermal and resonance cross sections and the other 68-group data.

The spectrum is calculated under the condition that the effective multiplication factor is equal to 1.0 by seeking the self consistent buckling (material buckling), instead of solving the eigenvalue problem with geometrical buckling.

Neutron scattering is, in practice, not isotropic and a convenient way of taking this into account in neutron transport calculation is to use the transport approximation. In the thermal energy region, the following form of transport approximation is recommended by Honeck[10]:

$$\Sigma_s^{g\to g'}=\Sigma_{s0}^{g\to g'}-\delta_{gg'}\Sigma_{s1}^{g}, \tag{8}$$

$$\Sigma_{s1}^{g}=\sum_{g'}\Sigma_{s1}^{g\to g'}, \tag{9}$$

where $\delta_{gg'}$ is the Kronecker δ-function, and $\Sigma_{s0}^{g\to g'}$ and $\Sigma_{s1}^{g\to g'}$ are isotropic and anisotropic parts of the scattering kernel, respectively. In the present work, Eq. (8) is used for all transport equations. To justify the validity of this procedure, a comparison with experiment on resonance integrals is shown in **Table 2**. The transport correction reduces the resonance integrals by 1.5 and 0.4 barn for the lattice of H_2O and D_2O coolant, respectively. The resonance integrals in Table 2 (Cal. 1) are in good agreement with the results by RICM[11] under the condition of narrow resonance approximation in moderator.

All the fundamental data used here derive from the RBU-library.

The above multigroup scheme has been programmed for HITAC-5020F as the computer code CLUSTER-III. Computing time is about 15 min for UO_2 fueled lattices, but about 25 min for PuO_2+UO_2 fueled lattices, as typical examples.

III. Comparison between Calculation and Experiment

The accuracy of the method of calculation is tested by comparing the results of calculation with experiment. The calculation gives detailed information on neutron flux in space and energy. The experiment, on the other hand, gives energy integrated quantities, the energy region being separated at most into two. If the theory correctly predicts neutron flux spectra, then the integrated or averaged quantities of neutron flux spectra should be correct. The converse of this statement is not true since the agreement of averaged pro-

Table 3 Dimensions and enrichment of lattices studied[13][14][17]

Lattice	Pitch (cm)	Fuel pin					Coolant void ratio (%)	Pressure tube		Calandria tube		Moderator R_{eff} (cm)
			Enrich (%)	r_f (cm)	$r_{s\,in}$ (cm)	r_s (cm)		$R_{p\,in}$ (cm)	$R_{p\,out}$ (cm)	$R_{c\,in}$ (cm)	$R_{c\,out}$ (cm)	
UO_2-D_2O-22.5	22.5(S)†	UO_2	1.5	0.75	0.7625	0.8425	0, 30, 100	5.8	6.1	6.6	6.75	12.650
UO_2-D_2O	25. (S)†	UO_2	1.5	0.75	0.7625	0.8425	30, 100	5.8	6.1	6.6	6.75	14.105
PuO_2-D_2O	25. (S)†	UO_2+PuO_2	NU+0.493†††	0.75	0.7625	0.8425	0, 30, 100	5.8	6.1	6.6	6.75	14.105
UO_2-H_2O	11.2 (h)††	UO_2	1.5	0.5	0.57	0.61	0, 80, 100	4.25	4.55	—	—	5.881

† S: square, †† h: hexagonal, ††† Weight % of PuO_2 to (PuO_2+UO_2)
r_f: Radius of fuel pin, $r_{s\,in}$: Inner radius of fuel sheath, r_s: Outer radius of fuel sheath

perties does not necessarily imply the correctness of the detailed distribution[12]. However, comprehensive comparison of various quantities of a lattice with different dependence on energy should provide an indication of the degree of accuracy of the method of calculation.

Here the following quantities are studied:

(1) Micro-parameters of lattices
(2) Reaction distribution in space
(3) Thermal disadvantage factor
(4) Thermal spectrum index
(5) Multiplication factor, or what is known as the four factors, which is a combination of the avove quantities.

The lattices studied here are four kinds of 28-pin clusters with various void ratios in light-water coolant, of various lattice pitches, various kinds of fuel (UO_2 or PuO_2-UO_2) and of moderator (heavy- or light-water). They are located in two regioned critical cores with surrounding driver region. Measurements are performed in the central unit lattice of each cluster lattice region. The void ratios in coolant vary from 0% void (filled with light-water in coolant passage) to 100% void (filled with air coolant). Intermediate void ratios are simulated with light- and heavy-water mixtures. The definition of effective void ratio is

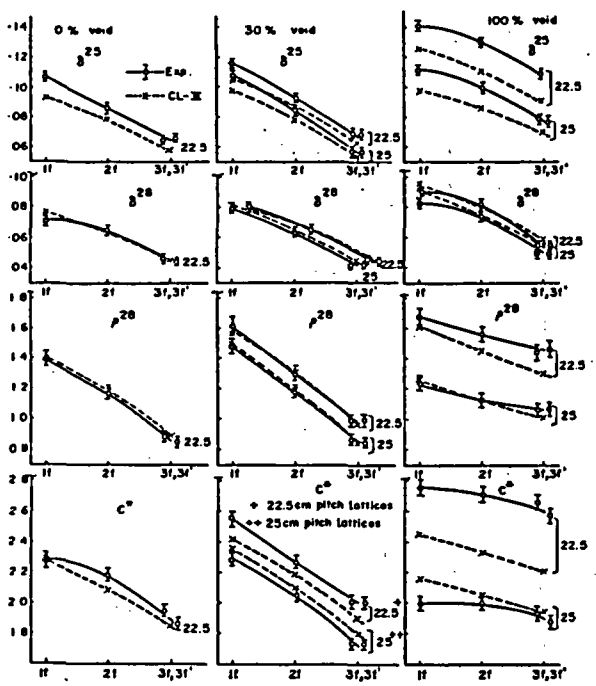

Fig. 2 Micro-parameters of UO_2-D_2O lattices

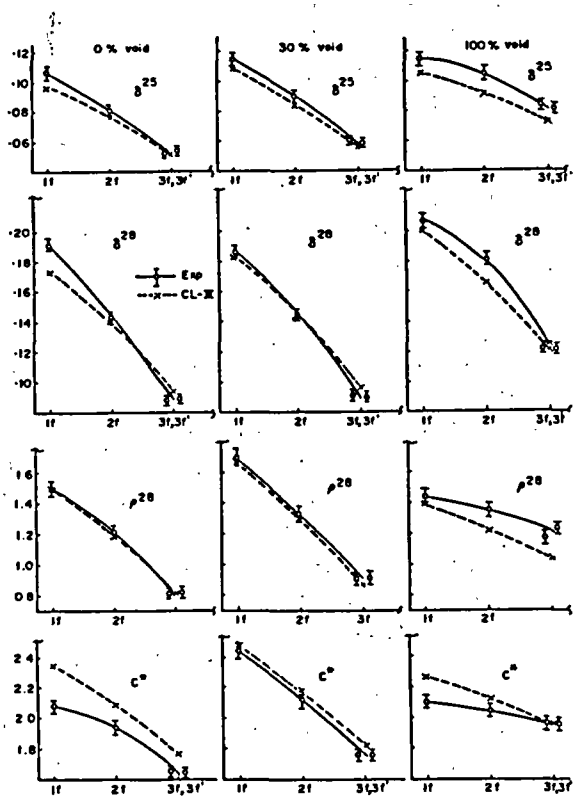

Fig. 3 Micro-parameters of PuO_2-D_2O lattices

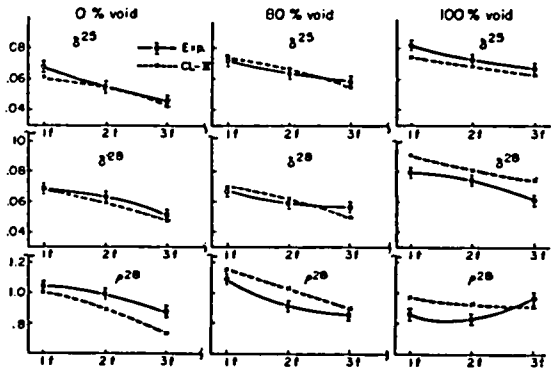

Fig. 4 Micro-parameters of UO_2-H_2O lattices

not the same for D_2O-30% lattices and for H_2O-80% lattice: in the D_2O-30% lattices it means the light-water volume ratio in coolant, but in the H_2O-80% lattice it denotes the effective light-water density of the mixture in reference to the absorption-to-scattering rate ratio. The necessary data for the calculation are listed in **Table 3**[13][14].

Figures 2~4 show the micro-parameters. The thermal cut-off energy E_c is set equal to the effective Cd cut-off energy, for which a value of 0.45 eV is used in all the lattices, considering the foil thickness used in the experiment[15]. In these figures the abscissa is the point in space where the measurement is made, for instance, 1f means the fuel of annulus 1 which corresponds to that of T-1 in Part (I) of the present series. From the discussion in Sec. II-2 of the present report, the calculation assumes that positions 3f and 3f′ are equivalent, although they are distinguished in the experiment.

Among the micro-parameters, δ^{28}, the ratio between the fast fission rate of ^{238}U and the total fission rate of ^{235}U, agrees well between measurement and calculation. Most of calculated results are within statistical error of the experiment. Since only the first few groups in the 69-group scheme contribute to the numerator of δ^{28}, the above mentioned results show that the corresponding part of the energy is correctly calculated relative to the thermal part.

The epi-to-thermal fission ratio of ^{235}U (δ^{25}) represents the epithermal neutron behavior relative to that of the thermal neutrons. Figures 2~4 show that the calculated value of δ^{25} is a little lower than that of experiment, especially for D_2O-lattices and in 100% void. The calculated value of RI_∞, the resonance integral for ^{235}U in infinite dilution, is 5% lower than by experiment (see Table 1). If this difference is corrected, the agreement becomes much better, almost within statistical error of the experiment. In the 100% voided D_2O-lattices, however, a 10% discrepancy still remains even after the correction. The calculated epi-to-thermal capture ratio of ^{238}U (ρ^{28}) at 3f in 100% void for the PuO_2-D_2O lattice is about 10% lower than experiment, but there is good agreement for the UO_2-D_2O lattice. Figure 2 shows that the resonance quantities δ^{25} and ρ^{28} are much more dependent on lattice pitch than is δ^{28}. This results from the fact that the moderator plays a more important role on resonance quantities. For the UO_2-H_2O lattices, the agreement of ρ^{28} is poorer, and the observed plots vary irregularly.

Lastly shown is the relative conversion ratio C^*, the ratio of the total capture rate of ^{238}U to the total fission rate of ^{235}U in the lattice relative to the same ratio in the thermal column. Calculation gives a 3~15% different value than experiment. Some discussions are given in Chap. IV

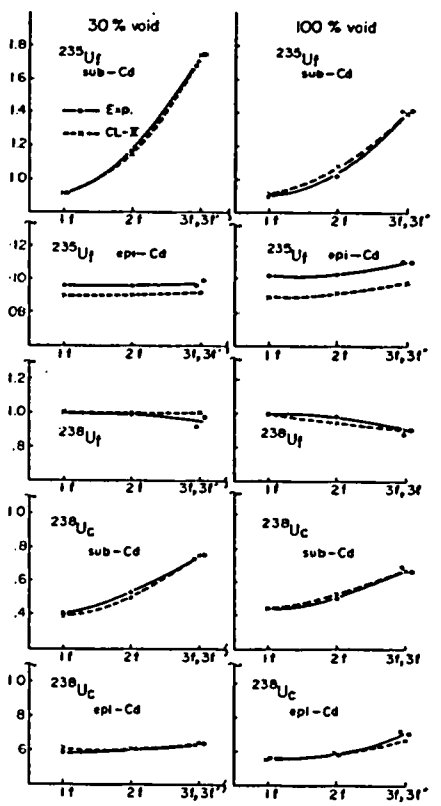

Fig. 5 Distribution of ^{235}U-fission, ^{238}U-fission and ^{238}U-capture (UO_2-D_2O lattices)

in this respect. In UO_2-H_2O lattices the quantity C^* has not been measured.

The micro-parameters directly relate to the multiplication factor (four factors). However, for the purpose of examining the accuracy of the method, of calculation, groupwise information on the reaction rates themselves, instead of the epi-to-thermal reaction rate ratios, should be more useful. **Figure 5** shows the distribution of ^{235}U-fission, ^{238}U-fission and ^{238}U-capture rates in UO_2-D_2O lattices. The reactions in Fig. 5 are normalized so as to give the unit value for the sum of epi- and sub-Cd contribution of each reaction at the position of the fuel in the annulus 1. The figure shows that all of the calculated distribution of reaction rates in each energy group agree well with measurement. For the Pu lattices similar comparisons are given in the Ref. (16).

Thermal disadvantage factors are given as average Dy reaction rate ratios in the homoid region (coolant, sheath and outside homogeneous annuli such as pressure tube, calandria tube and moderator) in reference to that of the average of all the fuel pins. The results are shown in **Table 4**[13][14][17]. For D_2O-lattices the disadvantage factors of coolant to fuel in each fuel annulus are also shown. The calculated disadvantage factor tends to be a little smaller than the measured. This tendency may come from the treatment based on the subcell model. (It must be remembered that the coolant region was partitioned into annuli in portions that differed between calculation and experiment. No correction has been made in this respect).

In **Table 5** the thermal spectrum index is given as Lu/Mn reaction rate ratios normalized to thermal column values. This is another important integral quantity of thermal flux showing the hardness of the thermal neutron spectrum. For UO_2 fueled lattices the calculated results are in good agreement with measured values. However for PuO_2-UO_2 fueled lattices, the calculations result in values somewhat lower than measurement in all space points and void ratios. Theoretically, the fact that the Lu/Mn reaction rate ratios are lower for PuO_2-UO_2 than for UO_2 fuel lattices is due to the large resonance of ^{239}Pu at 0.3 eV (see **Fig. 6**). However, the measured Lu/Mn reaction rate ratios in PuO_2-UO_2 fueled lattices are higher than in UO_2 fueled lattices even for those at the outer-most point of the moderator. It may suggest that effect of the

Table 4 Thermal disadvantage factor

	Lattice		UO_2-D_2O		PuO_2-D_2O			UO_2-H_2O		
	X	Void (%)	30	100	0	30	100	0	80	100
D.F. of region X in a unit cluster lattice	Sheath	Exp.	1.10±.03	—	1.13±.05	1.07±.05	1.03±.05	1.18	1.06	1.15
		CL-III	1.112	1.112	1.114	1.114	1.117	1.088	1.086	1.083
	Coolant	Exp.	1.246±.034	1.109±.033	1.33±.06	1.25±.06	1.11±.05	1.23	1.25	1.11
		CL-III	1.210	1.163	1.225	1.213	1.172	1.149	1.128	1.117
	PT	Exp.	2.16±.06	1.78±.05	2.42±.11	2.50±.11	1.70±.08	1.58	1.61	1.38
		CL-III	2.004	1.784	2.033	2.055	1.821	1.548	1.540	1.431
	CT	Exp.	2.17±.06	1.79±.06	2.48±.11	2.55±.12	1.81±.08	—	—	—
		CL-III	2.109	1.896	2.130	2.159	1.929			
	Mod.	Exp.	2.77±.14	2.81±.14	2.96±.13	3.28±.14	2.80±.14	2.03	2.28	2.12
		CL-III	2.837	2.818	2.867	2.961	2.934	2.001	2.132	2.089
D.F. of coolant in each ring X	1	Exp.	1.218±.025	1.040±.031	1.23±.06	1.11±.05	1.02±.05	—	—	—
		CL-III	1.204	1.120	1.228	1.217	1.138	1.149	1.121	1.091
	2	Exp.	1.236±.021	1.108±.033	1.31±.06	1.25±.06	1.06±.05	—	—	—
		CL-III	1.208	1.166	1.223	1.212	1.185	1.150	1.128	1.115
	3	Exp.	1.319±.041	1.187±.036	1.40±.06	1.31±.06	1.18±.05	—	—	—
		CL-III	1.212	1.171	1.227	1.214	1.189	1.150	1.130	1.122

Table 5 Thermal spectrum index $(\sigma^{Lu}/\sigma^{Mn})_x/(\sigma^{Lu}/\sigma^{Mn})_{\text{thermal column}}$

Position x	Lattice / Void (%)	UO_2-D_2O		PuO_2-D_2O			UO_2-H_2O		
		30	100	0	30	100	0	80	100
[1, f]	Exp.	1.38	1.57	1.45±.04	1.46±.04	1.56±.05	1.29	1.40	1.43
	CL-III	1.396	1.570	1.317	1.339	1.459	1.309	1.428	1.462
[2, f]	Exp.	1.36	1.49	1.43±.04	1.38±.04	1.47±.05	1.25	1.35	1.40
	CL-III	1.345	1.508	1.285	1.297	1.415	1.288	1.390	1.426
[3, f]	Exp.	1.28 1.28	1.34 1.35	1.32±.04 1.37±.04	1.33±.04 1.40±.04	1.42±.05 1.43±.05	1.21	1.29	1.39
	CL-III	1.293	1.410	1.242	1.255	1.345	1.250	1.319	1.372
Mod. (outermost)	Exp.	1.05	1.15	1.10±.03	1.18±.04	1.20±.04	1.03	1.08	1.09
	CL-III	1.104	1.133	1.098	1.104	1.130	1.095	1.108	1.119

spectral disturbance from the driver region is felt in the Lu/Mn reaction rate ratios, which are sensitive to the component of the spectrum.

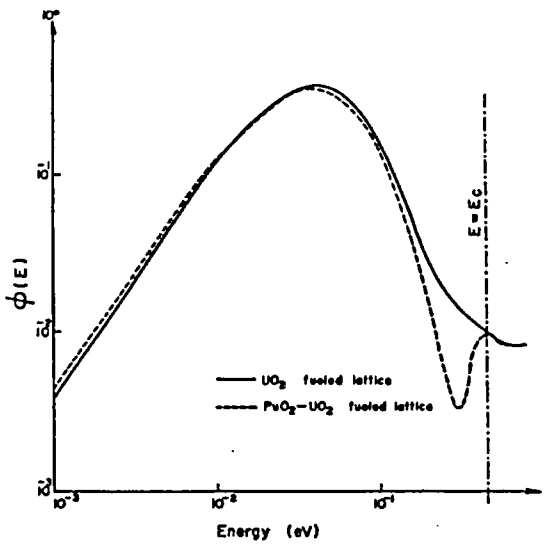

Fig. 6 Thermal neutron flux spectrum in a fuel pin at the innermost annulus of D_2O moderated 28-pin cluster lattices with 100% voided coolant

The multiplication factor can be determined from the micro-parameters and disavantage factors (see Appendix). In Fig. 7 comparisons are given between calculation and experiment on the fast effect ε, resonance escape probability p, thermal utilization factor f, and the multiplication factor k_∞, with various void ratios of coolant density*. For D_2O-lattices, the general tendency of the calculation to give lower values of resonance reaction than experiment, especially in the case of 100% voided lattices, results in a lower ε (owing to ^{235}U fission) and in higher p (owing to ^{235}U capture and ^{238}U capture). For the H_2O-lattice of 0% void the calculated resonance escape probability p is 2% higher than experiment. The discrepancy results mainly from the lower value of ρ^{28} especially at 3f. The discrepancy in the thermal disadvantage factor does not so severely affect the thermal utilization factor if the system embodies heavy-water moderator. For a system

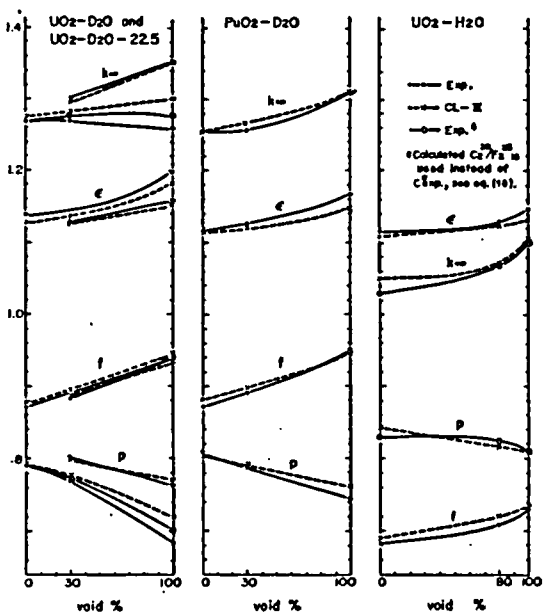

Fig. 7 Multiplication factor

* For UO_2-H_2O lattices $C_{exp}^* = C_{cal}^*$ is assumed, and for PuO_2-D_2O lattices, moreover, $\delta^{49'/25}$ and $\delta^{49'}$ (see Appendix) are used to obtain k_∞, of which no comparison has been given in this paper (see Ref. (16)).

with light-water moderator, however, the divergence more severely affects the thermal utilization and multiplication factors. The calculated multiplication factors k_∞ agree with experiment within 1%, except the cases of UO_2-D_2O-22.5 100% void and UO_2-H_2O 0% void, although some discrepancies in ε and p are cancelled out in k_∞. The void dependence of the multiplication factor is fairly well reproduced. For UO_2-D_2O-22.5 lattice of 100% void, half of the discrepancy between calculation and experiment in k_∞ results from the disagreement in C^*. For the UO_2-H_2O lattice of 0% void, the calculated k_∞ is larger than experiment by 2%, and this is due to the lower ρ^{28}.

IV. Discussion

Examining the void dependence of the four factors in cluster-type fuel lattices, it is seen from Fig. 7 that the multiplication factor has a tendency to rise with increasing void fraction. This results from the fact that coolant and moderator are separated from each other and that the void occurs only in the coolant. Generally the presence of void brings an advantage to the thermal utilization factor f (loss of absorber effect) and disadvantage to the resonance escape p (loss of slowing down effect).

In cluster lattices, neutrons are moderated mainly in the zone outside the fuel region. Even if the coolant becomes 100% void, neutrons pass into the fuel region from outside the moderator region. It results in less change of p with void in cluster lattices than in regular lattices (a numerical trial shows that the change of p in a cluster lattice is about one half that of a regular lattice). Since the change of p is smaller in cluster-type than in regular fuel lattices the repression effect is so much lower in the former type fuel lattices. Although moderation in coolant is of secondary importance in a cluster fuel lattice, it becomes more important as moderator-to-coolant volume ratio becomes smaller (compare two UO_2-D_2O lattices with different pitch in Fig. 7).

The loss of slowing-down effect also renders harder the thermal neutron spectrum in the fuel region. It reduces the advantage of f resulting from the loss of absorber effect. A numerical trial shows that the decrease of σ_{ath}^{235} with void in a cluster fuel lattice is about one half of that in a regular lattice, and that in some cases the thermal neutron spectrum in the fuel region of 100% void is softer than with other void fractions.

Comparisons between calculation and experiment have proved that the present method has a tendency to underestimate the micro-parameters such as δ^{25} and ρ^{28}, especially when the coolant becomes voided by 100%. The calculated neutron flux spectrum corresponds to the spectrum for a single region critical core whose configuration is the same as the test region (characteristic spectrum of the cluster lattice). On the other hand, the experimental lattices studied here are located at the center of the inner test region in two-region critical cores. Thus, in the experiment, the characteristic spectrum might be disturbed by the surrounding driver region.

A recent study[18] on the UO_2-D_2O cores indicated that the characteristic spectrum is realized in good approximation at the center of the test region if the spectrum is calculated under the assumption that the effective multiplication factor is equal to 1.0 (*cf.* self consistent buckling iteration method described in II-3 above). The four-group calculation of the study gives a 3% lower ϕ_3/ϕ_4 value than the characteristic spectrum at the center of the test unit lattice of UO_2-D_2O for 100% void and almost the same ϕ_3/ϕ_4 for other void percentages (for PuO_2-D_2O lattices a little larger disturbance may occur). This could prove useful for correcting the difference between the calculated and experimental values. In this connection, we recall the experimental verification reported in Part (I): It was there stated that in the test region the deviation of the observed spectrum from the characteristic is negligible.

Next, the Cd cut-off energy significantly affects such micro-parameters as where the fast-to-thermal reaction rate considered in small, and the reaction around the Cd cut-off energy is relatively important. For example, the changes of the values of δ^{25}, ρ^{28}, δ^{28} and C^* corresponding to a change of Cd cut-off energy from 0.45 eV to 0.625 eV, for example, were found by calculation to be about 10, 3, 1 and 1%, respectively. Among these parameters, δ^{25} is the most sensitive to Cd cut-off energy.

In the experimental analysis studied here the thermal cut-off energy is equal to the Cd cut-off energy of 0.45 eV. This might be considered

excessively low compared with the thermal cut-off energy generally used in multigroup calculations. A theoretical verification based on a simplified model shows that this value of thermal energy cut-off is still reasonable[20][21]. Moreover numerical calculation reveals that the effect of this treatment on the overall flux is small (less than 0.3% in k_∞) at least for the cases considered here.

The relative conversion ratio is expressed by

$$C_i^* = I_i\left(\frac{1+\rho^{28}}{1+\delta^{25}}\right)_i \qquad (10)$$

$$I_i = (C_2^{28}/F_2^{25})_i/(C_2^{28}/F_2^{25})_{\text{thermal column}}.$$

The notations used here are found in Appendix. The change of C_2^{28}/F_2^{25} depends on the thermal spectrum, so that the remaining independent information contained in C_i^* is I_i. Generally the value of I_i is 1.0 for the same spectrum at that in the thermal column, and exceeds 1.0 for harder spectra. This holds in calculation, but not for the I_i derived from experimentally determined values of ρ^{28}, δ^{25} and C^*. No successful explanation can here be given on this point.

The criterion of validity of the calculated flux distribution in the coolant is the thermal disadvantage factor. The calculated disadvantage factors of the coolant are lower than experiment, especially when the coolant is not voided, and are almost same for all fuel annuli. This is the result of adopting a subcell model in which an equal amount of coolant is attributed to all fuel pins. This model partitions the coolant in equal amounts to all fuel pins and locates the coolant nearer to the fuel pin than in actuality. Hence, the local water peaking becomes almost the same for all fuel annuli and lower than actual, giving a smaller disadvatage factor. The lower values of the coolant disadvantage factor reduce, in turn, the tube disadvantage factor. This is the limiting factor for the validity of the semi-analytical model used here. For the multiplication factor, however, the resulting effect is small for heavy-water moderated systems.

V. Conclusion

A study has been made on the neutron behavior in cluster-type fuel lattices to obtain information on neutron physics data directly from experiment (in Part (I) of this paper), and to develop a method of calculation, the validity of which being confirmed by comparison with experimental results.

In Part (II) of this paper a multigroup method of calculation has been proposed for cluster-type fuel lattices, using a semi-analytical treatment for calculating collision probabilities. The method has been compared comprehensively with experiments on micro-parameters, reaction distribution, thermal disadvantage factor, thermal spectrum index and multiplication factors. The studied lattices cover a range of parameters such as fuel material, lattice pitch, moderator material and void fraction.

The overall result has proved that the calculated values are generally in good agreement with experiment, though there is a tendency to give somewhat underestimated values for the resonance reaction. One of the reasons for this tendency may be the small deviation of spectrum from the characteristic, in the experimental system. Studies in single region cores are called for. In particular, more studies on Pu-fueled lattices are indispensable for ascertaining the accuracy of theories relating to burn-up calculations.

Acknowledgment

The authors are much indebted to Mr. H. Urushihara for preparing the computer code CLUSTER-III, and also to Mrs. Y. Inoue and Mrs. F. Fukunishi for writing parts of this code. The Power Reactor and Nuclear Fuel Development Corporation (PNC) is acknowledged for permission to publish the results of experiment and its analysis. Finally one of the authors (Yamamoto) wishes to thank Dr. S. Shima (former head of the Atomic Energy Division of Hitachi Central Lab.) for providing the occasion to initiate this work.

References

(1) Soodak, H., Sullivan, R.: *NDA*2131-38, (1961).
(2) Furuhashi, A., Yasukawa, S.: *JEARI-memo* 1656, (1964).
(3) Apliar, R.: *AEEW-R* 135, (1964).
(4) Yamamoto, K., Ishida, M.: *J. Nucl. Sci. Technol.*, 8(8), 458 (1971).
(5) Stace, R. H. W.: A review of the use of collision probabilities in lattice calculations, *Bournemouth Symp. Phys. Graphite Moderated Reactors*, (1962).

(6) HONECK, H. C.: *Nucl. Sci. Eng.*, 8, 193 (1960).
(7) NORDHEIM, L. W.: *ibid.*, 12, 457 (1962); NORDHEIM, L. W., KUNCIR, G. F.: *GA*-2527, (1961).
(8) MIZUTA, H., *et al.*: *JAERI*-1134, (1967).
(9) KOMATSU, I., FUKAI, Y.: *JAERI*-1105, (1966).
(10) HONECK, H. C.: *Nucl. Sci. Eng.*, 18, 49 (1964).
(11) MIZUTA, H., FUKAI, Y.: *J. Nucl. Energy*, 23, 589 (1969).
(12) HONECK, H. C., KAPLAN, I.: *Nucl. Sci. Eng.*, 8, 203 (1960).
(13) PNC-Rep. *SJ* 304 70 02-1~2 (1970); *SJ* 304 70 04-1~2 (1970); *SJ* 304 69 05-1~2 (1969); See also *J. Nucl. Sci. Technol.*, 9(11), 629 (1972).
(14) WAJIMA, J. T., *et al.*: *Hitachi Internal Rep.*, 6163 (1968); MITSUI, H., YAMAMOTO, K., WAJIMA, J. T., *et al.*: *Trans. ANS Winter Meeting*, (Washington), 589 (1970).
(15) TAKEDA, R., INOUE, K.: *J. Nucl. Sci. Technol.*, 1(5), 172 (1964).
(16) PNC-Rep. *SJ* 302 71-06, (1971).
(17) SHIMAMURA, A., KINOSHITA, M.: To be published.
(18) PNC-Rep. *SJ* 302 70-05, (1970).
(19) HELLSTRAND, E.: *J. Appl. Phys.*, 28, 1493 (1957).
(20) WEINBERG, A. M., WIGNER, E. P.: *"The Physical Theory of Neutron Chain Reactors"*, (1958), Univ. of Chicago Press.
(21) MATSUOKA, K.: *Hitachi Internal Rep.*, 3176 (1963).

[APPENDIX]

Experimentally, energy is separated at most into two regions: epi-Cd and sub-Cd, corresponding respectively to energies above and below the Cd cut-off energy. Thus in the present work, the four-factor formula is expressed with the quantities based on the two-group scheme, although this treatment obscures somewhat the traditional distinction between fast fission and resonance escape probabilities.

If Pu exists in the system, then the following parameters must be added as Pu micro-parameters:

$$\delta^{49'}=\frac{\text{Epi-Cd fission in Pu}}{\text{Sub-Cd fission in Pu}},$$

where 49′ means the summation of all isotopes of Pu, and

$$\delta^{49'/25}=\frac{\text{Total fission in Pu}}{\text{Total fission in }^{235}\text{U}}.$$

(1) Multiplication factor and four factors

$$k_\infty=\varepsilon p\eta f \tag{A1}$$

(2) Fast fission factor

$$\varepsilon=1+\frac{(\nu\Sigma_f)_1\phi_1}{(\nu\Sigma_f)_2\phi_2}=1+\frac{\delta^{25}+(\nu^{28}/\nu^{25})\delta^{28}(1+\delta^{25})+(\nu^{49'}/\nu^{25})\delta^{49'}[F_2^{49'}/F_2^{25}]}{1+(\nu^{49'}/\nu^{25})[F_2^{49'}/F_2^{25}]}, \tag{A2}$$

$$\text{where } [F_2^{49'}/F_2^{25}]=\delta^{49'/25}\frac{1+\delta^{49'}}{1+\delta^{25}} \tag{A3}$$

(3) Resonance escape probability

$$p=\frac{\Sigma_r}{\Sigma_r+\Sigma_{a1}}=\frac{1}{1+fP_2R}, \tag{A4}$$

$$R=\rho^{28}\frac{(1+\alpha_1^{28})^{-1}+(1+\alpha_1^{25})\delta^{25}/\rho^{28}[F_2^{25}/C_2^{28}]+(1+\alpha_1^{49'})\delta^{49'}/\rho^{28}[F_2^{49'}/C_2^{28}]+A_1^{\text{non fuel}}/C_1^{28}}{1+(1+\alpha_2^{25})[F_2^{25}/C_2^{28}]+(1+\alpha_2^{49'})[F_2^{49'}/C_2^{28}]}, \tag{A5}$$

$$\text{where } [F_2^{25}/C_2^{28}]=\frac{1+\rho^{28}}{1+\delta^{25}}\cdot\frac{1}{CR}, \tag{A6}$$

$$[F_2^{49'}/C_2^{28}]=\frac{1+\rho^{28}}{1+\delta^{49'}}\cdot\frac{\delta^{49'/25}}{CR} \tag{A7}$$

Here, CR is the conversion ratio (total capture rate of ^{238}U to total fission rate of ^{235}U), P_2 the non-escape probability of sub-Cd neutrons, and α the capture-to-fission ratio.

(4) Thermal utilization factor and η

$$f^{-1}=1+\underset{i\neq f}{S}\frac{V_i\Sigma_{a2}^i}{V_{\text{fuel}}\Sigma_{a2}^{\text{fuel}}}(\sigma_{\text{Dy}}^{\text{fuel}}/\sigma_{\text{Dy}}^i)[DF_i(\text{Dy})] \tag{A8}$$

$$\eta=(\overline{\nu\Sigma_f})_2/\Sigma_{a2}^{\text{fuel}}$$

The calculated value is generally used for η.

Journal of NUCLEAR SCIENCE and TECHNOLOGY, 9 (12), p. 716~720 (December 1972).

Preparation of Uranium-233

Tomitaro ISHIMORI, Kaoru UENO, Kan KIMURA, Michio HOSHI, Masakatsu SAEKI, Akira SAITO, Masaharu ASANO, Johkun AKATSU and Bruno LEUGGER†

*Japan Atomic Energy Research Institute**

Received June 5, 1972

Thorium dioxide amounting to 1.3kg was irradiated for 241 days at an average neutron flux of 6×10^{10} n/cm²·sec, and allowed to stand for 1.2yr. This cooling lowered the γ-activity of the irradiated ThO_2 sufficiently to permit handling without special shielding. Nine milligrams of ^{233}U were extracted with TBP in dodecane, and determined by α-ray counting. The mass ratio of the uranium isotopes obtained was determined by mass spectrometry. It was indicated that the ^{233}U was contaminated with natural uranium.

KEYWORDS: *uranium 233, irradiation, preparation, thorium dioxide, mass spectrometry, neutron flux, solvent extraction, TBP, alpha radiation counting, Japan Power Demonstration Reactor, neutron beams*

I. INTRODUCTION

The fertile nuclear materials ^{238}U and ^{232}Th exist on earth in large quantities, compared with the fissile material ^{235}U. It is thus thought that these fertile materials should play an important role in the large scale nuclear power generation expected in the future.

The preparation of very small quantities of ^{233}U by irradiation of gram amounts of Th target has previously been reported by the authors[1][2].

The present study aims at preparing ^{233}U with relatively small quantities of fission products (F.P.) by irradiating large amounts of Th in a reactor for long periods under low neutron flux. About 1.3 kg of ThO_2 was thus irradiated for 241 days at an average thermal neutron flux of 6×10^{10} n/cm²·sec, and allowed to stand for 1.2yr. The γ-ray activity of the sample was reduced sufficiently to permit its handling without special shielding. From this sample, 9mg of ^{233}U was obtained by extraction with TBP in dodecane, and determined by α-ray counting. Mass spectrometric measurement revealed that the ^{233}U was contaminated with natural uranium. Technical considerations for the production of ^{233}U are also discussed.

II. EXPERIMENTAL

1. Target Assembly

Three assemblies of target materials were prepared, each assembly containing 0.43kg of Th in the form of ThO_2 pellets. The pellets were cylindrical—12.5mm in outside diameter and 10.5 mm long. Each pellet contained 11.1g of ThO_2 on the average. The pellets were packed into Zircaloy cladding tubes, which were then sealed by welding. The target assembly is shown in **Photo. 1.**

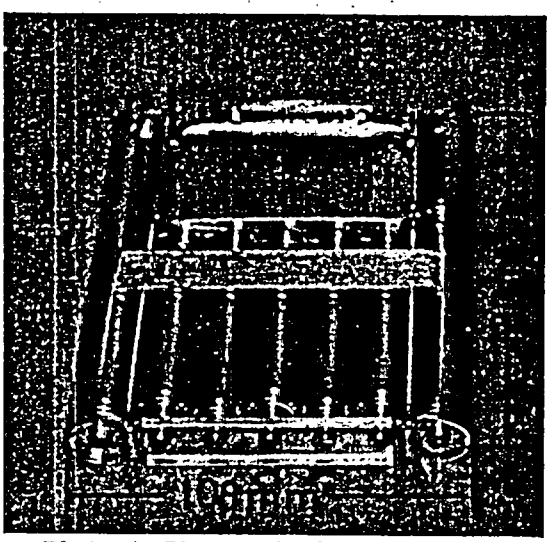

Photo. 1 Photograph of target assembly

2. Measurement of the Thermal and Fast Neutron Fluxes

The $^{59}Co(n,\gamma)^{60}Co$ and $^{54}Fe(n,p)^{54}Mn$ reactions

† IAESTE exchange student from Bern University (1969).

*. *Tokai-mura, Ibaraki-ken.*